Detailed 2-D imaging of growth and burst of edge-localized filaments in KSTAR H-mode plasmas*

M.J. Choi[1], G.S. Yun[1], J. Lee[1], W. Lee[1], H.K. Park[1],
C.W. Domier[2], N.C. Luhmann[2], B. Tobias[3], A.J.H. Donné[4], J.H. Lee[5], and KSTAR team[5]

[1] *POSTECH, Pohang, Republic of Korea*

[2] *University of California at Davis, Davis, U.S.A.*

[3] *Princeton Plasma Physics Laboratory, Princeton, U.S.A.*

[4] *FOM-Institute for Plasma Physics Rijnhuizen, Nieuwegein, The Netherlands*

[5] *National Fusion Research Institute, Daejeon, Republic of Korea*

Introduction

Edge-Localized Modes (ELMs) [1] are a class of semi-periodic edge instabilities in H-mode tokamak plasmas causing loss of edge confinement, which can lead to a severe damage on the first wall of ITER-relevant tokamaks. Previous observations have revealed many important features such as the filamentary nature of the ELM perturbation, the detachment or burst of the filaments from the last closed flux surface (LCFS) and the radial expansion of the detached filaments in the scrape-off region [2]. The peeling-ballooning theory [3] is generally accepted as the physical mechanism for the onset of the ELMs. Despite the significant progress in understanding the ELM physics, several important issues regarding the growth and burst of the ELM filaments are still unclear due to the lack of diagnostics to capture the mode dynamics inside the pedestal region. In particular, the burst of the ELM filaments, which presumably involves non-linear physics, has not been observed in detail yet.

ECEI system

In 2010 KSTAR campaign, the entire ELM evolution process has been observed in detailed 2-D images using an Electron Cyclotron Emission Imaging (ECEI) system [4]. Growth and burst stages of the ELM filaments were identified and a strong poloidal flow was observed.

The ECEI system is a heterodyne microwave camera for observation of ECE intensity (T_*) in 2-D poloidal plane. Due to the difficulty of absolute calibration, the ECEI images in this paper are presented as 2-D pictures of the relative T_* fluctuations ($\delta T_*/\bar{T}_*$). The KSTAR ECEI system has dual detector arrays, enabling simultaneous measurements of high and low field side. A total of $24(\text{vertical}) \times 8(\text{radial}) = 192$ channels constitute each side with the channel separation $\sim 1-2$ cm in both directions.

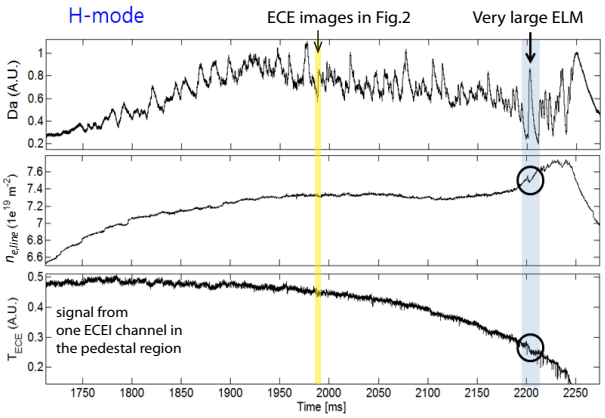

Figure 1: Typical KSTAR H-mode plasma (# 4431). The peaks in D_α line emission (from the lower divertor region) correspond to the ELM crashes. Note that the relatively large drop in the pedestal ECE intensity and the line integrated density at the large ELM event near $t = 2200$ ms.

2-D observation of ELM filaments

Fig.1 shows the time traces of D_α emission, ECE (pedestal), and line integrated density ($n_{e,\mathrm{line}}$) during the ELMy period of a typical KSTAR H-mode plasma (# 4431). The small and large spikes in the D_α trace indicate the relative amplitude of the ELM crash events. For large ELM events, $n_{e,\mathrm{line}}$ drops by a few percents and the pedestal ECE intensity drop by ~ 10 % whereas small ELM events show negligible change.

Before discussing the ECEI images, it should be noted that the optical depth is the key parameter for the localization of ECE measurement as well as for the proportionality between T_* and T_e. The optical depth τ of the pedestal region will be thick or gray ($\tau \gtrsim 1$) assuming the kinetic profiles $T_e = 500 - 200$ eV and $n_e = 2 - 0.2 \times 10^{19}$ m^{-3}, which ensures the local ECE measurement [5]. However, the optical depth is not large enough to guarantee the equality $\delta T_*/\bar{T}_* = \delta T_e/\bar{T}_e$. Instead, $\delta T_*/\bar{T}_*$ depends on the density fluctuation $\delta n_e/\bar{n}_e$ as well as $\delta T_e/\bar{T}_e$ [6], which makes difficult the accurate interpretation of $\delta T_*/\bar{T}_*$.

The detailed dynamics of the ELM filaments has been analyzed using the LFS ECEI images for a typical large ELM event. Fig.2 shows the time trace of a pedestal ECEI channel (marked as a white cross in the first ECEI image). The time period (a) includes the initial growth phase and the saturated state, and the time period (b) and (c) correspond to the burst phase.

The initial growth phase is illustrated by the first three images of Fig.2a. As clearly shown in the images, the spatially localized filaments emerge inside the LCFS (red bold line). Note that the flux surfaces (dotted black lines) estimated by an equilibrium reconstruction are an approximate visual aid only. The filaments, presumably formed along the magnetic field, grow in amplitude and size. The fully developed size is ~ 5 cm both in radial and poloidal directions.

The apparent poloidal velocity V^*_{pol} of the ELM filaments is counter-clockwise (positive in our sign convention) as indicated by the yellow arrows following one filament. The poloidal motion of the filaments is a combined effect of both poloidal and toroidal flow according to the relation

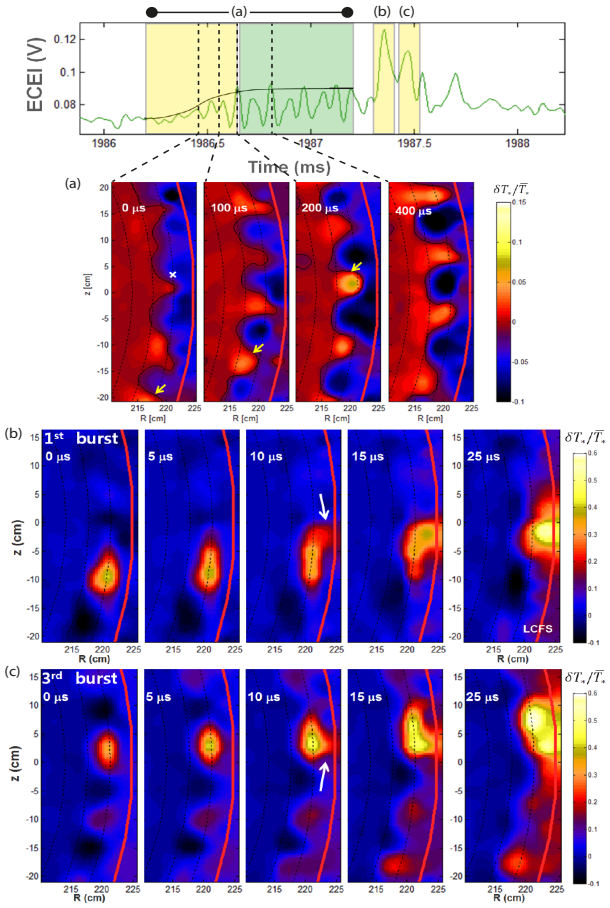

Figure 2: Time trace of a pedestal ECEI signal during a large ELM event and the corresponding ECEI images [7]. (a) Initial growth phase (the first yellow box in the time trace) and saturated state (the green box). (b) The first ELM filament burst in a series of four similar bursts. The arrow indicates the finger-like structure triggering the burst. (c) The third burst of the same filament, $\sim 150\ \mu$s later.

$V^*_{pol} = V_{pol} - V_{tor} \times \tan\alpha$, where α is the pitch angle of the magnetic field line (Fig.3). V^*_{pol} would be always negative (clockwise) if V_{pol} is zero. The observed positive (counter-clockwise) $V^*_{pol} \sim 1$ km/s implies that V_{pol} must be finite and positive. V_{pol} will be ~ 4 km/s using $V_{tor} = 50$ km/s estimated from a charge exchange spectroscopy measurement and $\alpha \sim 3.5^o$ [7].

The last image of Fig.2a represents the saturated state of the ELM filaments. In this state, the filament does not grow in size and intensity on the average. This state usually appears in case of large ELMs, and often followed by a transient period where the filaments almost disappear from the ECEI window and then re-emerge with a reduced poloidal mode number.

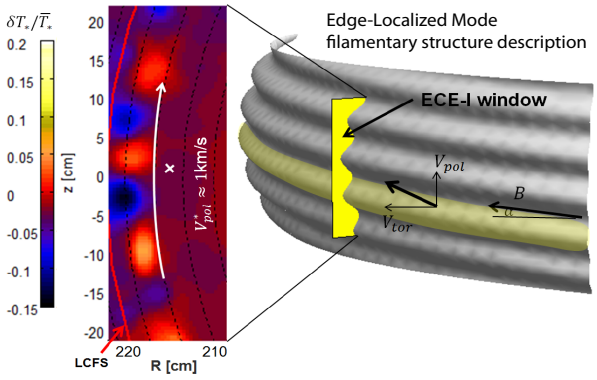

Figure 3: Poloidal flow of the filamentary ELM structure. The filaments with net poloidal and toroidal velocities pass by the laboratory-fixed LFS ECEI view, making the apparent flow in the upward direction in the ECEI view.

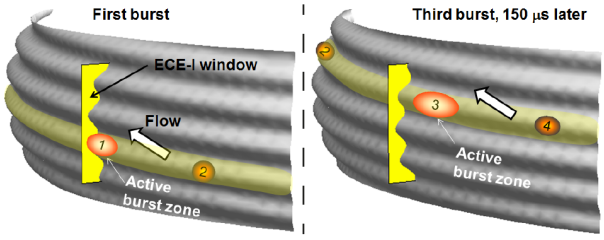

Figure 4: The phenomenological model [7] for the multiple bursts shown in the Fig.2b and 2c. The localized burst zones of the filament are depicted. Note that the filament has both poloidal and toroidal velocities.

Fig.2b is the first in a series of bursts of one ELM filament. The poloidal mode number has been decreased (larger poloidal separation) compared to that of the initial growth phase. The filament has grown in amplitude and elongates poloidally prior to the burst (first two images). A finger-like structure develops and touches the LCFS in the third image. The ECE intensity increase in the outer region (i.e., scrape-off layer) in the next images indicates the fast heat/particle flux from the burst zone through the finger. The heat/particle transport is convective and sustained for ~ 50 μs, which is similar to the pressure-driven localized burst and collective heat transport in the sawtooth crashes [8]. Three similar bursts of the same filament follow for a few hundred μs, releasing all the remaining excess heat/particle (Fig.2c). A phenomenological model for the multiple bursts is described in Fig.4, which shows the multiple localized burst zones formed along the filament [7].

In summary, the growth and burst of the ELM filaments have been studied in the pedestal region using the ECEI images of KSTAR ELMy H-mode plasma. The filamentary structure inside the LCFS, the poloidal and toroidal flows, and the dynamic stages of the ELM evolution have been described.

* This work was supported by the NRF Korea, the US DOE, and the Association Euratom-FOM.

References

[1] J. W. Connor, *Plasma Phys. Control. Fusion* **40**, 191 (1998)

[2] A. Kirk *et al.*, *Phys. Rev. Lett.* **96**, 185001 (2006)

[3] P. B. Snyder *et al.*, *Plasma Phys. Control. Fusion* **46**, A131 (2004)

[4] G. S. Yun *et al.*, *Rev. Sci. Instr.* **81**, 10D930 (2010)

[5] M. Bornatici *et al.*, *Nucl. Fusion* **23**, 1153 (1983)

[6] C. Janicki, *Nucl. Fusion* **33**, 3 (1993)

[7] G. S. Yun *et al.*, *Phys. Rev. Lett.*, accepted for publication

[8] H. K. Park *et al.*, *Phys. Rev. Lett.* **96**, 195003 (2006)